

Cite this: *Dalton Trans.*, 2013, **42**, 13723

Synthesis of bis(*N*-arylcarboximidoylchloride)pyridine cobalt(II) complexes and their catalytic behavior for 1,3-butadiene polymerization†

Heng Liu,^{a,b} Xiangyu Jia,^{a,b} Feng Wang,^{a,b} Quanquan Dai,^a Baolin Wang,^a Jifu Bi,^a Chunyu Zhang,^a Liping Zhao,^a Chenxi Bai,^a Yanming Hu^{*c} and Xuequan Zhang^{*a}

A new family of bis(*N*-arylcarboximidoylchloride)pyridine cobalt(II) complexes with the general formula [2,6-(ArN=CCl)₂C₅H₃N]CoCl₂ (Ar = 2,4,6-Me₃C₆H₂, **4a**; 2,6-ⁱPr₂C₆H₃, **4b**; 2,6-Me₂C₆H₃, **4c**; C₆H₅, **4d**; 4-Cl-2,6-Me₂C₆H₂, **4e**) and a typical Brookhart–Gibson-type reference complex [2,6-(2,4,6-Me₃C₆H₂N=CMe)₂-C₅H₃N]CoCl₂ (**5a**) were synthesized and characterized. Determined by X-ray crystallographic analysis, complexes **4a**, **4c–e**, and **5a** adopted a trigonal bipyramidal configuration, and **4b** adopted a distorted square pyramidal geometry. In combination with ethylaluminum sesquichloride (EASC), all the complexes were highly active towards 1,3-butadiene polymerization, affording polybutadiene with predominant *cis*-1,4 content (up to 96%). **4a** with chlorine atoms at the imine groups exhibited higher catalytic activity than did **5a**, indicating that the incorporation of chlorine atoms into the ligand improves the activity. The activity of the complexes in 1,3-butadiene polymerization was in the order of **4a** > **4c** ~ **4e** ~ **4b** > **4d**, which is consistent with the trend of spatial opening degree around the metal center in the complexes as revealed by crystallographic data. Screening polymerization conditions proved that EASC was the most efficient among the cocatalysts examined.

Received 29th May 2013,
Accepted 15th July 2013

DOI: 10.1039/c3dt51403j

www.rsc.org/dalton

Introduction

The stereospecific polymerization of 1,3-dienes has been highlighted in both academic and industrial domains in the past few decades due to the myriad of applications of polydienes.¹ The endeavor to design novel metal complexes makes available numerous precursors based on transition metals (Ti,² Fe,³ Ni,⁴ Co,⁵ etc.) and rare earth metals.⁶ Among them, Co-based catalysts become increasingly attention-grabbing because polybutadienes with versatile microstructures⁷ can be afforded, including *cis*-1,4 and syndiotactic 1,2- moieties, depending on catalyst formulation.

Since the discovery of bis(arylimino) pyridine Co(II) complexes as effective catalysts for the ethylene polymerization and oligomerization, a variety of well-defined transition metal

complexes through modifying the parent ligand framework have been designed and explored in the field of olefin polymerization.⁸ Much work is also in progress on aspects of 1,3-diene polymerization. For instance, bis(benzimidazolyl)-amine cobalt(II) dichloride/MAO is an efficient system to afford polybutadiene with high *cis*-1,4 stereoregularity.⁹ 2-Arylimino-6-(alcohol)pyridine nickel(II)¹⁰ and bis(oxazolonyl)pyridine chromium(III)¹¹ complexes are reported to be highly *cis*-1,4 or *trans*-1,4 selective in 1,3-butadiene polymerization. We found that cobalt and iron complexes supported by bis(arylimino)pyridine ligands afforded polybutadienes having high *cis*-1,4 or *trans*-1,4 contents depending on the metal centre and the ligand environment.¹²

As mentioned above, Brookhart–Gibson-type bis(arylimino)pyridine and its derivatives are well-known ligands for transition metal complexes due to the ease of tuning their catalytic performance by modifying the ligand backbone.¹³ The nature of substituents of the ligand has a great influence on the catalytic behavior of the complex in olefin and 1,3-diene polymerization. Generally speaking, three modification sites are available on the ligand skeleton of the typical Brookhart–Gibson-type catalyst (Scheme 1). For instance, the transition-metal complexes ligated by bis(arylimino)pyridine with chlorine, *t*-butyl, and nitro groups at *para*-position of the pyridyl ring (site 1) exhibit rather different polymerization behaviors.¹⁴

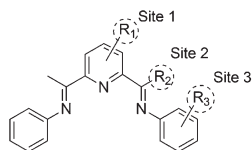
^aChangchun Institute of Applied Chemistry, Chinese Academy of Sciences, 5625 Renmin Street, Changchun 130022, PR China. E-mail: xqzhang@ciac.jl.cn; Fax: +86 8526 2307; Tel: +86 431 8526 2303

^bGraduate School of the Chinese Academy of Sciences, Beijing 100039, PR China

^cDepartment of Polymer Science and Engineering, School of Chemical Engineering, Dalian University of Technology, Dalian 116024, PR China.

E-mail: ymhu@dlut.edu.cn; Fax: +86 411 8498 6101; Tel: +86 431 8526 2303

†Electronic supplementary information (ESI) available. CCDC 872215, 903515, 903516, 903517, 941866 and 941867. For ESI and crystallographic data in CIF or other electronic format see DOI: 10.1039/c3dt51403j



Scheme 1 Three main modification sites on the typical bis(arylimino)pyridine ligand framework.

Various substituents such as fluorineamine,¹⁵ *meta*-fluorinated aryls,¹⁶ ferrocenyl groups,¹⁷ and other aniline analogs¹⁸ have been introduced into the iminophenyl ring of the ligand (site 3); it was found that the steric and electronic properties of these aniline analogs had a significant influence on olefin polymerization. Interestingly, the incorporation of electron-withdrawing substituents into site 3 enhances the activity of the complexes for olefin polymerization.¹⁹ In contrast, studies regarding site 2 are fairly limited.²⁰ Previous reports described the synthesis of a series of transition metal complexes ligated by bis(arylimino)pyridine bearing electron-donating groups ($-OR$, $-SR$, $-NR_2$, *etc.*) at site 2 and found that the nature of the heteroatom plays an important role in governing the catalytic activity in ethylene polymerization. Thus, it is reasonable to speculate that the incorporation of electron-withdrawing groups will also exert a large effect on the catalytic activity. In the present study, the electron-withdrawing chlorine atom was introduced into site 2; due to its proximity to $C=N$, it is expected that the electropositive character of the cobalt centre will be enhanced; therefore, a higher catalyst activity will be attained.

In the following content, we deal with the synthesis of bis(*N*-arylcarboximidoylchloride)pyridine cobalt(II) complexes and their catalytic behavior for 1,3-butadiene polymerization along with the typical Brookhart–Gibson-type ketimine cobalt(II) complex for comparison. Furthermore, the influences of the substituent of the ligand and polymerization conditions on the polymerization of 1,3-butadiene were investigated in detail.

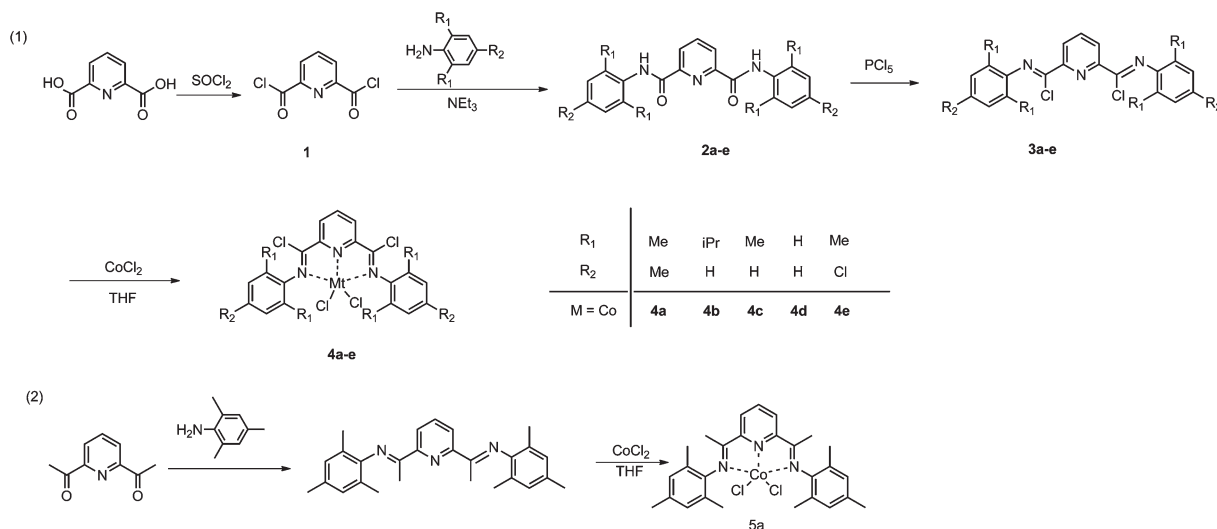
Results and discussion

Synthesis and characterization of the ligands and corresponding cobalt(II) complexes

The ligands **3a–e** containing chlorine atoms at the imine carbon and different substituents at the *ortho*- and/or *para*-position of the phenyl ring were prepared with high purity in good yields according to Scheme 2. Complexes of **4a–e** and **5a** were prepared by the treatment of the corresponding ligands with 1.0 equivalent of anhydrous $CoCl_2$ in dry THF. The ligands and complexes were identified by 1H NMR, ^{13}C NMR, IR, and elemental analysis.

In the IR spectra, absorption bands of the imine $C=N$ in complexes **4a–e** appear at 1614 – 1627 cm^{-1} , which are obviously red shifted in comparison with the corresponding ligand (1650 – 1660 cm^{-1}), indicating that the nitrogen atoms of imines coordinated to the central metal as donors. The structures of **4a–e** and **5a** were further confirmed by a single X-ray crystallographic study; selected bond lengths and angles are summarized in Table 2. The molecular structures are shown in Fig. 1 and 4.

Crystals of **4a** and **5a** suitable for X-ray structure determination were obtained by slow diffusion of pentane into their CH_2Cl_2 solutions, and the molecular structures are shown in Fig. 1. Both **4a** and **5a** are closer to C_s symmetry about a plane containing cobalt, two chlorines, and a pyridyl nitrogen atom. The coordination geometries at the cobalt metal center can be best described as distorted trigonal bipyramidal with the equatorial plane formed by the pyridyl nitrogen atom and the two chlorine atoms, and the other two $Co-N(C=N)$ bonds positioned in the axial direction. In both complexes: (1) the $Co-N(C=N)$ bond is clearly longer than that of the $Co-N(\text{pyridyl})$ bond; (2) the cobalt atom deviates slightly from the N_3 plane, 0.125 Å for **4a** and 0.064 Å for **5a**, respectively; (3) the pyridine ring is inclined slightly with respect to the N_3 plane, *ca.* 4.1° in **4a** and *ca.* 5.6° in **5a**, respectively; (4) the planes of the phenyl



Scheme 2 Synthesis of complexes **4a–4e** and **5a**.

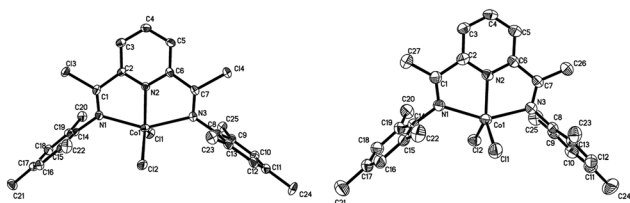


Fig. 1 ORTEP view of complex **4a** and **5a**, drawn at 35% of probability; hydrogen atoms and methylene chloride are omitted for clarity.

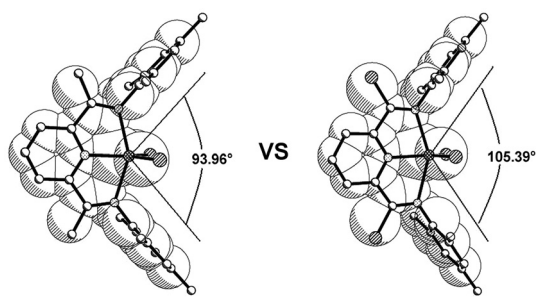


Fig. 2 The spanned angles between two phenyl rings in **5a** (left) and **4a** (right).

rings are oriented essentially orthogonally to the plane of the N_3 plane, 88.86° and 82.00° for **4a**, 87.50° and 88.72° for **5a**, respectively. On the other hand, the bond lengths of $C=N$ in **4a** [$C(1)-N(1)$: $1.250(8)\text{ \AA}$ and $C(7)-N(3)$: $1.270(7)\text{ \AA}$] are shorter than those in **5a** [$1.280(5)\text{ \AA}$ and $1.289(5)\text{ \AA}$, respectively], and the bond distances of $Co(1)-N(1)$ and $Co(1)-N(3)$ in **4a** [$2.303(5)$ and $2.405(4)\text{ \AA}$, respectively] are considerably longer than those in **5a** [$2.263(4)$ and $2.229(4)\text{ \AA}$, respectively], indicating an enhanced electropositivity of the cobalt(II) center in **4a**.²¹ Introducing chlorine atoms into the ligand, the spanned angle between the two phenyl rings in **4a** is 105.39° , which is much larger than that in **5a** (93.96°) (Fig. 2). Meanwhile, the angles of $Co(1)-N(1)-C(14)$ [$129.1(4)^\circ$ (**4a**) vs. $126.2(3)^\circ$ (**5a**)] and $Co(1)-N(3)-C(8)$ [$131.8(4)^\circ$ (**4a**) vs. $126.2(3)^\circ$ (**5a**)] become larger in **4a**. These results suggest that **4a** exhibits a more open, *i.e.* a sterically less congested coordination sphere around the metal center (Fig. 3), allowing easier accessibility for 1,3-butadiene molecules.

The molecular structures of **4b**, **4c**, **4d** and **4e** are shown in Fig. 4. **4b** has an approximate C_s molecular symmetry about the plane containing the cobalt atom, and its geometry at the metal center can be best described as distorted square pyramidal with $Cl(1)$ as the apical position. The four basal atoms (three nitrogen atoms and one chlorine atom $Cl(2)$) are nearly coplanar with the $Cl(2)$ atom deviating only 0.120 \AA out of the N_3 plane. The two $Co-Cl$ bond lengths are almost the same (2.2592 \AA and 2.2209 \AA , respectively). The $Co-N(\text{pyridyl})$ bond distance [$2.0662(17)\text{ \AA}$] is clearly shorter than that of $Co-N(C=N)$ [$2.2645(68)\text{ \AA}$]. The two $C=N$ bonds have a typical double-bond character with a bond length of $1.263(5)\text{ \AA}$ and $1.251(5)\text{ \AA}$, respectively. The pyridine ring inclines with respect

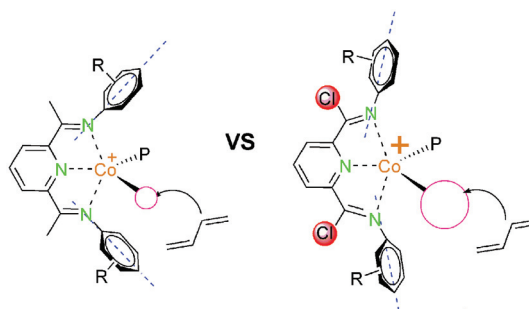


Fig. 3 Explanatory drawings that **4a** (right) exhibits an enhanced electropositivity and more spatial opening degree than **5a** (left). (The size of plus sign "+" stands for the intensity of electropositivity at the Co centre; the size of pink circle "O" stands for the space of the coordination sphere for 1,3-butadiene; "P" stands for the polybutadienyl chain.)

to the N_3 plane only by 1.27° , suggesting that the N_3 structure and the pyridine are nearly coplanar. The deviation of the cobalt atom from the N_3 plane was 0.549 \AA , which is clearly larger than that of **4a**. The spanned angle between the two phenyl rings in **4b** is 99.67° , and the angles of $Co(1)-N(1)-C(14)$ and $Co(1)-N(3)-C(8)$ are $125.96(13)^\circ$ and $125.80(13)^\circ$, respectively.

Solid structures of **4c**, **4d**, and **4e** are isomorphous, having approximate C_s symmetry about a plane formed by the cobalt atom, the two chlorine groups, and the pyridyl nitrogen atom. The coordination geometries around the cobalt atoms can be best described as distorted trigonal bipyramidal with the equatorial planes formed by the two chlorine atoms, the pyridyl nitrogen atom, and the other two axial $Co-N(C=N)$ bonds. The deviations of the Co atoms from N_3 planes in **4c**, **4d**, and **4e** are 0.010 , 0.026 , and 0.048 \AA , respectively, indicating a nearly coplanar structure. Two phenyl rings in complexes **4c** and **4e** are oriented nearly orthogonal to the plane of the N_3 plane, 88.79° and 86.52° in **4c**, 82.89° and 78.54° in **4e**, respectively; however, for **4d**, the two dihedral angles are

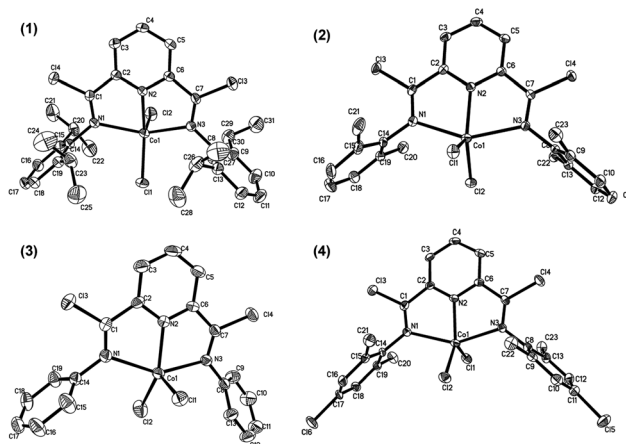


Fig. 4 ORTEP view of complexes **4b**(1), **4c**(2), **4d**(3), and **4e**(4), drawn at 35% of probability; hydrogen atoms and methylene chloride are omitted for clarity.

89.53° and 55.52°, the latter one is much smaller than the others.

Variation of the substituents on the phenyl rings of the ligand leads to significant environmental differences (mainly spatial opening degree) around the metal centre (Table 1). Complex **4a** bearing 2,4,6-trimethyl groups possessed the largest C(14)–N(1)–Co(1) and C(8)–N(3)–Co(1) bond angles (129.1(4) and 131.8(4)°, respectively), giving the 1,3-butadiene monomer the best accessibility to the cobalt centre. Changing the *ortho*-position substituents from isopropyl to hydrogen, an order of **4c** > **4b** > **4d** was observed. Introduction of a chlorine atom to the *para*-position of the phenyl ring results in a reduction of C(14)–N(1)–Co(1) and C(8)–N(3)–Co(1) bond angles when comparing with **4c** (126.0(3)° vs. 129.44(12)°; 126.7(3)° vs. 127.20(13)°). The smallest C(14)–N(1)–Co(1) and C(8)–N(3)–Co(1) bond angles (123.8(2)° and 122.7(2)°, respectively) are found in the case of **4d** affording the worst 1,3-butadiene accessibility to the cobalt centre.

1,3-Butadiene polymerization behavior of the cobalt(II) complexes

The complexes activated with EASC were examined for the polymerization of 1,3-butadiene, and the results are

Table 1 Different spanned angles around the metal centre

Complex	C(14)–N(1)–Co(1) (°)	C(8)–N(3)–Co(1) (°)
4a	129.1(4)	131.8(4)
4b	125.80(13)	125.96(14)
4c	129.44(12)	127.20(13)
4d	123.8(2)	122.7(2)
4e	126.0(3)	126.7(3)

Table 2 Selected bond lengths (Å) and angles (°) of complexes **4a–e** and **5a**

	4a	5a	4b	4c	4d	4e
Bond lengths (Å)						
Co(1)–N(1)	2.303(5)	2.263(4)	2.2469(18)	2.3182 (16)	2.258(3)	2.251 (3)
Co(1)–N(2)	2.033(5)	2.042(4)	2.0662(17)	2.0562 (16)	2.051(3)	2.042 (3)
Co(1)–N(3)	2.405(4)	2.229(4)	2.2822(18)	2.3001 (17)	2.215(3)	2.302 (3)
Co(1)–Cl(1)	2.2457(17)	2.2586(15)	2.2209(7)	2.2473 (6)	2.2917(14)	2.2522 (12)
Co(1)–Cl(2)	2.2286(17)	2.2762(14)	2.2592(7)	2.2477 (6)	2.2308(14)	2.2264 (12)
N(1)–C(1)	1.250(8)	1.280(5)	1.257(3)	1.262 (2)	1.251(5)	1.259 (5)
N(1)–C(14)	1.452(7)	1.443(6)	1.453(3)	1.450 (2)	1.434(4)	1.443 (5)
N(2)–C(6)	1.343(7)	1.355(5)	1.342(3)	1.341 (2)	1.339(5)	1.342 (5)
N(2)–C(2)	1.348(7)	1.344(6)	1.329(3)	1.343 (3)	1.354(5)	1.341 (5)
N(3)–C(7)	1.270(7)	1.289(5)	1.260(3)	1.263 (3)	1.263(5)	1.264 (5)
N(3)–C(8)	1.421(7)	1.450(6)	1.449(3)	1.446 (3)	1.435(5)	1.443 (5)
Bond angles (°)						
N(1)–Co(1)–N(2)	76.03(18)	74.59(15)	74.39(6)	74.92 (6)	75.04(11)	75.85 (13)
N(1)–Co(1)–Cl(1)	97.79(13)	99.79(10)	97.58(5)	99.16 (4)	96.45(9)	97.21 (9)
N(1)–Co(1)–Cl(2)	98.98(13)	95.29(10)	100.43(5)	98.03 (4)	98.01(9)	100.57 (9)
N(2)–Co(1)–N(3)	73.93(17)	75.70(16)	73.44(7)	74.72 (6)	75.54(12)	74.61 (13)
N(2)–Co(1)–Cl(1)	109.28(14)	119.76(11)	147.06(6)	114.39 (5)	101.84(10)	103.65 (10)
N(2)–Co(1)–Cl(2)	127.10(14)	95.29(10)	93.36(5)	130.81 (5)	142.73(10)	136.11 (10)
N(3)–Co(1)–Cl(1)	96.10(11)	96.89(10)	98.21(5)	96.98 (4)	98.67(9)	97.29 (9)
N(3)–Co(1)–Cl(2)	95.60(12)	99.20(10)	101.57(5)	98.57 (5)	99.59(9)	95.19 (9)
N(1)–Co(1)–N(3)	149.64(17)	150.19(14)	141.75(7)	149.36 (6)	149.08(11)	149.41 (12)
Co(1)–N(1)–C(14)	129.1(4)	126.2(3)	125.80(13)	129.44 (12)	123.8(2)	126.0 (3)
Co(1)–N(3)–C(8)	131.8(4)	126.2(3)	125.96(14)	127.20 (13)	122.7(2)	126.7 (3)
C(1)–N(1)–C(14)	120.7(5)	119.3(4)	122.24(19)	129.44 (12)	124.6(3)	122.4 (4)
C(7)–N(3)–C(8)	119.9(5)	119.4(4)	122.18(19)	121.62 (17)	124.3(3)	122.4 (4)

summarized in Table 3. Complex **4a** bearing 2,4,6-trimethyl groups on the phenyl ring of the ligand exhibited the highest activity; the conversion reached 97% in 20 minutes. It is clear from Fig. 5 that the catalyst activity of **4a** is obviously higher than that of its chlorine-free counterpart **5a** during the whole polymerization process. This result might be attributable to the higher electropositivity and a more open spatial structure²² of the metal center in **4a** as revealed by the crystallographic data, which facilitates the monomer coordination. Complexes **4b** and **4c** having isopropyl and methyl substituents at the 2,6-position of the phenyl ring of the ligand are found to be more active than the unsubstituted analogue **4d**. **4e** bearing methyl groups and chlorine atom at the 2,6-position and 4-position of the phenyl ring exhibited nearly the same activity as those of **4b** and **4c** due to their similar spatial structure (for **4b**, **4c**, and

Table 3 1,3-Butadiene polymerization with Co(II) complexes bearing different ligand environments

Run ^a	Complex	Yield (%)	$M_n \times 10^{-4}$ ^b	M_w/M_n ^b	Microstructure ^c (%)		
					<i>Cis</i> -1,4-	<i>Trans</i> -1,4-	1,2-
1	4a	97.0	14.5	3.1	93.1	3.6	3.3
2	5a	92.0	14.5	2.9	93.9	3.0	3.1
3	4b	93.1	13.6	3.0	92.0	4.0	4.0
4	4c	93.7	17.8	2.6	94.5	2.7	2.8
5	4d	71.8	31.1	2.7	96.0	1.6	2.4
6	4e	93.6	15.2	3.2	94.4	2.7	2.8
7	CoCl ₂	3.1	—	—	97.6	1.4	1.0

^a Polymerization conditions: at 20 °C for 20 min; precursor 12.3 μmol, 1,3-butadiene 37 mmol, [Al]/[Co] = 50, EASC, toluene 20 mL.

^b Determined by GPC eluted with THF (polystyrenes as standards).

^c Determined by IR and NMR.

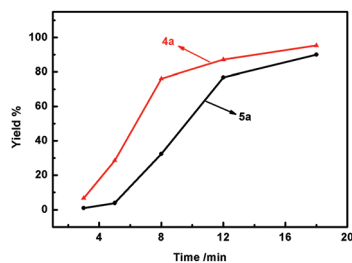


Fig. 5 Plots of the relationship between polymer yield and polymerization time with **4a** and **5a** as precatalysts.

4e, the average Co–N(C=N)–C bond angle approximated 126.8° and the average difference did not exceed 1.5°). Thus, the activity of the complexes in the polymerization of 1,3-butadiene is in the order of **4a** > **4c** ~ **4e** ~ **4b** > **4d**, which is consistent with the trend in the spatial opening degree of the ligand in the complex as mentioned above. Similar results were observed in the cases of Co(II) complexes bearing bis-(benzimidazolyl)amine ligands; that is, more open spatial structure of the metal center results in higher catalytic activity.²³

The molecular weight and *cis*-1,4 selectivity significantly changed with the variation of the ligand environment. Solely changing the *ortho*-position substituents from ⁱPr- to H-, an obvious increment in both *cis*-1,4-content and M_n was observed. These results may be correlated to the spatial opening degree around the cobalt metal centre; with an increment of spatial congestion near the cobalt centre, the chain termination process could be efficiently suppressed giving rise to a remarkable jump from 13.6×10^4 (**4b**) to 31.1×10^4 (**4d**) in M_n . As for the stereoselectivity, the *cis*-1,4 content of poly(1,3-butadiene) obtained with **4b** bearing *ortho*-isopropyl was 92%, and slightly increased for **4c** bearing less bulky *ortho*-methyl groups. The highest *cis*-1,4 selectivity of 96% was observed in the case of **4d** without substituents. It seems that narrowing the spatial opening degree favors the formation of *cis*-1,4 content. Similar results were observed for the alkylphosphine cobalt(II) complex.²⁴ In the case of CoCl₂, the catalyst system

afforded polybutadiene with a high *cis*-1,4 content (97.6%) but in a much lower yield (3.1%).

With the complex **4a**/EASC catalyst system, the effects of reaction parameters such as the polymerization temperature, the [Al]/[Co] ratio, and the cocatalyst type on the catalytic activities and polymer microstructures were further examined (Table 4). Similar to most transition metal-based catalysts, the Co complexes also suffered from the decay of catalytic activity at elevated polymerization temperature.^{10,25} In the present study, the catalyst gave the polymer in a low yield (14.8%) at 0 °C. The optimum activity (97%) was gained at 20 °C, and further increasing the temperature resulted in a decreased catalytic activity. It is worth noting that the present catalyst exhibited a high activity affording 70% yield even at 80 °C, indicating the high thermal stability of the active species. The M_n of the polymer decreased as the temperature increased, and meanwhile, the M_w/M_n increased from 1.6 to 5.2, which might be due to the facilitated chain transfer reaction at the elevated temperature. GPC curves obtained at different temperatures are shown in Fig. S1 in ESI,[†] from which it was clearly observed that the peaks shifted towards the low molecular weight fraction along with a gradual broadening molecular weight distribution as the temperature increased. Fig. 6 shows the variation of microstructures of the polybutadiene obtained at different temperatures. The polymer obtained at 0 °C had a high *cis*-1,4 content of 98.5% and negligible 1,2- and *trans*-1,4-contents. The *trans*-1,4 and 1,2- contents of the polymer gradually increased at the expense of *cis*-1,4 selectivity with the polymerization temperature increasing. The polymer obtained at 80 °C is composed of 76.8% *cis*-1,4, 12.5% *trans*-1,4, and 10.7% 1,2-contents. Fig. 7 provides the NMR spectra obtained in runs 9 and 12, from which we could clearly observe an increase in *trans*-1,4 and 1,2- contents in run 12 when compared with run 9. In principle, the terminal π -allylic unit of the polymer chain can be coordinated in the *anti*- or *syn*- conformation to the metal centre, the *anti*- isomer gives rise to *cis*-1,4 and 1,2-polymerization, while the *syn*- isomer causes *trans*-1,4- and 1,2-polybutadiene formation. At lower temperature, most of the

Table 4 1,3-Butadiene polymerization with **4a** under different polymerization conditions

Run ^a	Polymerization conditions			Yield (%)	$M_n \times 10^{-4}$	M_w/M_n^d	Microstructure ^e (%)		
	Al ^c	Al/Co	T (°C)				<i>Cis</i> -1,4	<i>Trans</i> -1,4	1,2-
8		50	0	14.8	32.2	1.6	98.5	0.8	0.7
9		50	20	97.0	14.5	3.1	93.1	3.3	3.6
10		50	40	93.7	7.81	4.6	87.7	6.6	5.7
11	EASC	50	60	89.2	5.93	4.4	83.6	8.6	7.8
12		50	80	70.0	4.52	5.2	76.8	12.5	10.7
13		15	20	89.0	12.59	2.7	91.7	6.0	2.3
14		80	20	100	13.08	2.5	94.0	4.3	1.6
15		100	20	95.0	10.23	2.9	93.0	4.9	2.1
16	MAO ^b	50	20	73.5	13.60	3.4	94.9	2.8	2.3
17	TEA ^b	50	20	2.0	—	—	—	—	—
18	TIBA ^b	50	20	1.3	—	—	—	—	—

^a Polymerization conditions: precursor 12.3 μ mol; 1,3-butadiene 37 mmol; polymerization time 20 min, toluene 20 mL. ^b Polymerization time: 4 h. ^c EASC: ethylaluminum sesquichloride; MAO: methyl aluminoxane; TEA: triethylaluminium; TIBA: triisobutylaluminium. ^d Determined by GPC eluted with THF (polystyrene as standards). ^e Determined by IR and NMR.

monomers formed *cis*-1,4 polybutadiene through path 1 (Scheme 3) due to the hypothesis that the newly formed double bonds helped stabilize the active species through π -back-bonding and it was more kinetically favored. With the increasing of temperature, *anti-syn* isomerization through the π - σ -rearrangement was gradually facilitated owing to the reason that the *syn*- isomer was thermodynamically more stable, which led to an increment of *trans*-1,4 and 1,2- contents (paths 3 and 4). DSC was done to investigate the influence of microstructure on the glass transition temperature T_g , and the data and spectra are provided in Fig. S3.† Polybutadiene

obtained at 0 °C performed the lowest T_g (−102.95 °C); increasing the temperature from 20 to 80 °C, T_g increased monotonously from −101.48 °C to −94.74 °C, indicating that the microstructures influenced significantly the T_g of polybutadienes.

On the other hand, the catalytic activity increased gradually with an increasing ratio of [Al]/[Co], reaching complete conversion at [Al]/[Co] = 80. With the variation of the [Al]/[Co] ratio, no conspicuous changes in M_n and MWD of polymers were observed, suggesting that EASC was not an efficient chain transfer agent at 20 °C for the present system.

Since the cocatalyst plays an important role in transition metal catalyzed polymerization, the polymerization of 1,3-butadiene was carried out by employing different cocatalysts. Among the cocatalysts examined, EASC is the most efficient, affording the polymer in a high yield (97%) in 20 minutes with high *cis*-1,4 content (93.1%). Using MAO as a cocatalyst, the catalytic activities towards 1,3-butadiene polymerization decreased, and the polymer yield was 73.5% in 4 h. In the cases of TEA and TIBA, the activities were negligible (2.0% and 1.3% yield, respectively), which means that they are less effective for activation of the complex than EASC and MAO. Similar results were observed in the polymerization of 1,3-butadiene with other Co-based catalytic systems.²³

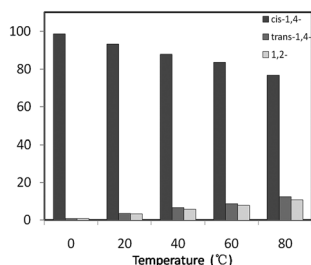


Fig. 6 Changes in the microstructures of PBDs with the variation of reaction temperature.

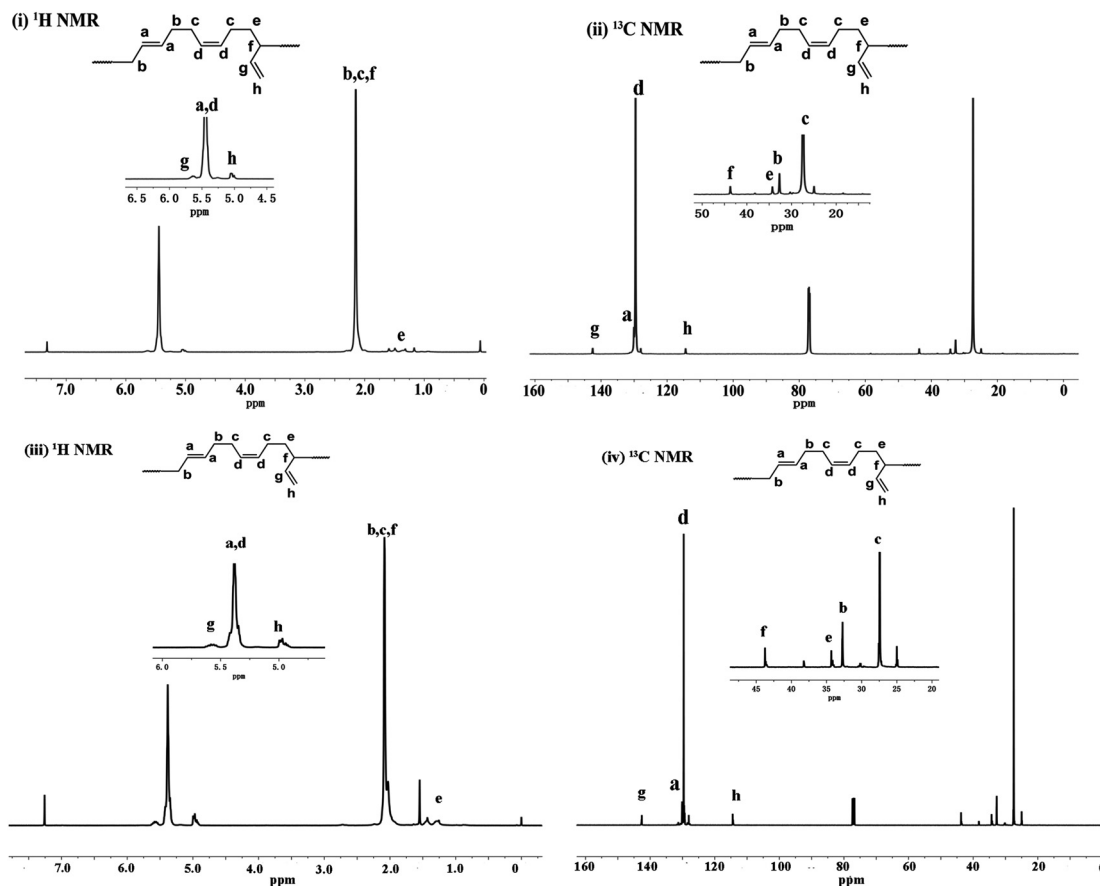
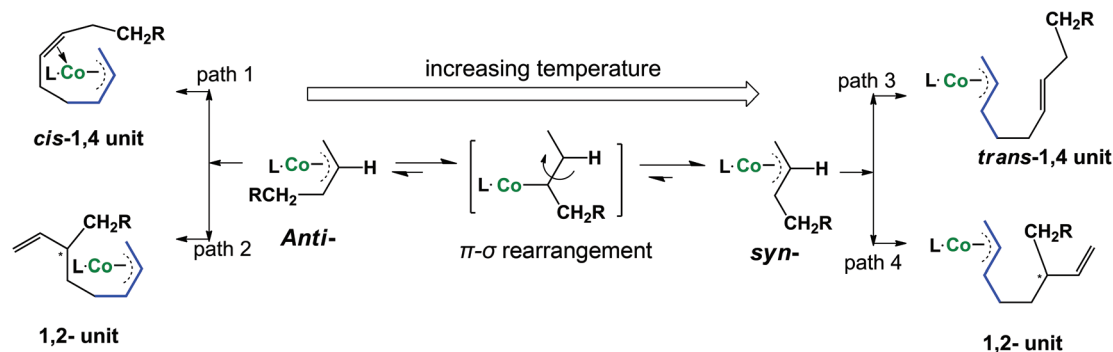


Fig. 7 NMR spectra of the poly(1,3-butadiene)s obtained by the 4a/EASC system. Run 9: (i) and (ii); run 12: (iii) and (iv).



Scheme 3 Proposed scheme for 1,3-butadiene polymerization. (Blue lines stand for the newly incorporated monomer.)

Conclusions

A series of cobalt(II) complexes supported by bis(*N*-arylcaboximidoylchloride)pyridine **4a–e** were synthesized and fully characterized. As determined by X-ray crystallographic analysis, the complexes adopted distorted trigonal bipyramidal and square pyramidal configurations. In combination with EASC, all the complexes afforded polybutadienes in high yields ranging from 72% to 97% with a high *cis*-1,4 content (up to 96%). Incorporation of chlorine atoms into the imine groups of the ligand enhanced the catalytic activity of the complexes for 1,3-butadiene polymerization. The substituent of the phenyl ring of the ligand affected the activity of the complex, and the activity decreased in the order of **4a** > **4c** ~ **4e** ~ **4b** > **4d**, which is consistent with the trend of spatial opening degree as revealed by the crystallographic data. With the bulkiness of the substituent on the phenyl ring decreasing, the *cis*-1,4 content of the resulting polybutadiene increased. The catalytic activity of the complex decreased as the polymerization temperature increased, while the polymer yield remained 70% even at 80 °C, indicating the high thermal stability of the formed active species.

Experimental

General considerations

All manipulations were carried out under a nitrogen atmosphere in a glove box. The solvents were refluxed over CaH₂ or sodium-benzophenone and distilled prior to use. 1,3-Butadiene was obtained from Lanzhou Petrochemical Company. Other chemicals were commercially available and used without further purification.

¹H NMR (400 MHz) and ¹³C NMR (100 MHz) spectra were recorded using a Varian Unity spectrometer in CDCl₃ at ambient temperature using tetramethylsilane as an internal standard. FTIR spectra were recorded using a BRUKER Vertex-70 FTIR spectrometer. Elemental analysis was performed using an elemental Vario EL spectrophotometer. The proportion of *cis*-1,4 and *trans*-1,4 units of the polymer was determined by FTIR spectra, ¹H NMR, and ¹³C NMR. The molecular weights (*M_n*) and molecular weight distributions (*M_w*/*M_n*) of polymers were measured at 30 °C by gel permeation

chromatography (GPC) equipped with a Waters 515 HPLC pump, four columns (HMW 7 THF, HMW 6E THF × 2, HMW 2 THF), and a Waters 2414 refractive index detector. Tetrahydrofuran was used as the eluent at a flow rate of 1.0 mL min⁻¹. The values of *M_n* and *M_w*/*M_n* were determined using polystyrene calibration.

Preparation and characterization of ligands and complexes

All the bis(*N*-arylcaboximidoylchloride)pyridine cobalt(II) dichloride complexes were prepared in the same manner; a typical synthesis of complex **4a** is described as follows:

2,6-Pyridinedicarboxylic acid (5.0 g, 30 mmol) and thionyl chloride (30 mL) were added to a flask; the reaction mixture was refluxed with stirring for 24 h under a nitrogen atmosphere until a homogenous brown solution was obtained. The remaining unreacted thionyl chloride was removed by distillation under reduced pressure, and a light pink powder of 2,6-pyridine carbonyl dichloride was obtained. Yield, 6.1 g (100%). The product was moisture sensitive and used directly in the next procedure.

A solution of 2,6-pyridine carbonyl dichloride (6.1 g, 30 mmol) in 50 mL CH₂Cl₂ was added dropwise into a solution of 2,4,6-trimethylaniline (8.11 g, 60 mmol) and triethylamine (8.36 mL, 60 mmol) in CH₂Cl₂ (100 mL). The reaction mixture was refluxed for 6 h under a nitrogen atmosphere, then the reaction mixture was washed with water and brine, and the organic layer was dried over anhydrous magnesium sulfate. After CH₂Cl₂ was evaporated, the solid was recrystallized from toluene and dried under vacuum at 50 °C to give the product **2a** as a white solid. Yield, 10.95 g (91.0%). ¹H NMR (400 MHz, CDCl₃, δ, ppm): 9.02 (s, 2H, NH), 8.51 (d, 2H, Pyr-*H_m*), 8.14 (t, 1H, Pyr-*H_p*), 6.95 (s, 4H, Ar-H), 2.30 (s, 6H, Ar-C_pH₃), 2.26 (s, 12H, Ar-C_oH₃). ¹³C NMR (100 MHz, CDCl₃, δ, ppm): 161.6, 148.8, 139.3, 137.1, 134.8, 130.5, 128.9, 125.5, 20.9, 18.4. FT-IR (KBr; cm⁻¹): 3005, 2971, 1683, 1661, 1509, 1230, 1160, 1073, 1003, 848, 647. Anal. calc. for C₂₅H₂₇N₃O₂ (401.5): C, 74.79; H, 6.78; N, 10.47. Found: C, 74.73; H, 6.81; N, 10.42.

2a (5 g, 12.46 mmol), phosphorous pentachloride (PCl₅, 5.19 g, 24.92 mmol), and 200 mL CH₂Cl₂ were added into a flask. After reflux for 3 h with stirring, the volatiles were removed under vacuum, and the remains were extracted with hexane. The hexane solution was kept at -40 °C and yellow crystals were obtained. After washing with hexane and drying

under vacuum at 50 °C, product **3a** was obtained. Yield, 2.44 g (44.6%). ¹H NMR (400 MHz, CDCl₃, δ, ppm): 8.49 (d, 2H, Pyr-*H_m*), 8.01 (t, 1H, Pyr-*H_o*), 6.94 (s, 4H, Ar-H), 2.32 (s, 6H, Ar-C_PH₃), 2.10 (s, 12H, Ar-C_OH₃). ¹³C NMR (100 MHz, CDCl₃, δ, ppm): 151.2, 145.2, 143.4, 137.6, 134.0, 128.6, 125.8, 125.6, 20.8, 17.8. FT-IR(KBr; cm⁻¹): 302, 2969, 1656, 1508, 1471, 1202, 1139, 898, 850, 611, 551. Anal. calc. for C₂₅H₂₅Cl₂N₃ (439.4): C, 68.49; H, 5.75; N, 9.59. Found: C, 68.41; H, 5.72; N, 9.55.

A solution of **3a** (0.44 g, 1.0 mmol) in 5 mL THF was added dropwise to a suspension of anhydrous CoCl₂ (0.13 g, 1 mmol) in 3 mL THF, the reaction mixture was stirred for 6 h and a green suspension was formed. The precipitate was filtered and dried under vacuum at 40 °C and the desired product **4a** was obtained. Yield, 0.40 g (70.2%). A single crystal of **4a** was obtained by layering *n*-pentane on their dichloromethane solutions at room temperature. FT-IR (KBr; cm⁻¹): 3064, 2919, 1626, 1540, 1483, 1327, 1140, 1078, 853, 818. Anal. calc. for C₂₅H₂₅Cl₄CoN₃ (568.2): C, 52.84; H, 4.43; N, 7.39. Found: C, 52.90; H, 4.51; N, 7.37.

[N,N'-Bis(2,6-diisopropylphenyl)pyridine-2,6-carboximidoyl dichloride (3b)]. Yield, 4.88 g (75%). ¹H NMR (400 MHz, CDCl₃, δ, ppm): 8.52 (d, 2H, Pyr-*H_m*), 8.03 (t, 1H, Pyr-*H_o*), 7.20–7.26 (m, 6H, Ar-H), 2.82 (hept, 4H, -CH(CH₃)₂), 1.19 (d, 24H, -CH(CH₃)₂). FT-IR(KBr; cm⁻¹): 3070, 2960, 1650, 1443, 1180, 910(m), 794, 757, 624. Anal. calc. for C₃₁H₃₇Cl₂N₃ (522.6): C, 71.25; H, 7.14; N, 8.04. Found: C, 71.20; H, 7.13; N, 8.09.

[N,N'-Bis(2,6-dimethylphenyl)pyridine-2,6-carboximidoyl dichloride (3c)]. Yield, 3.12 g (61%). ¹H NMR (400 MHz, CDCl₃, δ, ppm): 8.51 (d, 2H, Pyr-*H_m*), 8.02 (t, 1H, Pyr-*H_o*), 7.02–7.13 (m, 6H, Ar-H), 2.14 (s, 24H, -CH₃). ¹³C NMR (100 MHz, CDCl₃, δ, ppm): 150.9, 145.8, 145.3, 135.0, 128.2, 127.7, 127.1, 124.5, 17.8. FT-IR(KBr; cm⁻¹): 3024, 2977, 1655, 1595, 1471, 1282, 1189, 1086, 993, 775, 689, 495. Anal. calc. for C₂₃H₂₁Cl₂N₃ (410.3): C, 67.32; H, 5.16; N, 10.24. Found: C, 67.29; H, 5.18; N, 10.25.

[N,N'-Bisphenylpyridine-2,6-carboximidoyl dichloride (3d)]. Yield, 0.22 g (5%). ¹H NMR (400 MHz, CDCl₃, δ, ppm): 8.40 (d, 2H, Pyr-*H_m*), 7.98 (t, 1H, Pyr-*H_o*), 7.10–7.50 (m, 10H, Ar-H). FT-IR (KBr; cm⁻¹): 3062, 1660, 1552, 1446, 1203, 915, 886, 757, 699, 630. Anal. calc. for C₁₉H₁₃Cl₂N₃ (354.3): C, 64.42; H, 3.70; N, 11.86. Found: C, 64.32; H, 3.79; N, 11.89.

[N,N'-Bis(4-chloro-2,6-dimethylphenyl)pyridine-2,6-carboximidoyl dichloride (3e)]. Yield, 3.76 g (63%). ¹H NMR (400 MHz, CDCl₃, δ, ppm): 8.50 (d, 2H, Pyr-*H_m*), 8.03 (t, 1H, Pyr-*H_o*), 7.11 (s, 4H, Ar-H), 2.11 (s, 12H, -CH₃). ¹³C NMR (100 MHz, CDCl₃, δ, ppm): 150.8, 145.2, 144.1, 137.6, 129.4, 127.8, 127.7, 125.6, 17.6. FT-IR (KBr; cm⁻¹): 3075, 2983, 1652, 1469, 1442, 1192, 986, 914, 828, 805, 616. Anal. calc. for C₂₃H₁₉Cl₄N₃ (479.3): C, 57.64; H, 4.00; N, 8.75. Found: C, 57.59; H, 4.05; N, 8.78.

[N,N'-Bis(2,6-diisopropylphenyl)pyridine-2,6-carboximidoyl dichloride] CoCl₂ (4b)]. Yield, 0.56 g (85.3%). FT-IR (KBr; cm⁻¹): 3071, 2959, 1614, 1578, 1465, 1382, 1164, 1083, 801, 765. Anal. calc. for C₃₁H₃₇Cl₄CoN₃ (652.4): C, 57.07; H, 5.72; N, 6.44. Found: C, 57.12; H, 5.73; N 6.38.

[N,N'-Bis(2,6-dimethylphenyl)pyridine-2,6-carboximidoyl dichloride] CoCl₂ (4c)]. Yield, 0.42 g (77.8%). FT-IR (KBr;

cm⁻¹): 3075, 2973, 1627, 1587, 1468, 1172, 1081, 955, 842, 775, 734. Anal. calc. for C₂₃H₂₁Cl₄CoN₃ (540.18): C, 51.14; H, 3.92; N, 7.78. Found: C, 51.19; H, 3.98; N, 7.81.

[N,N'-Bisphenylpyridine-2,6-carboximidoyl dichloride] CoCl₂ (4d)]. Yield, 0.21 g (44.5%). FT-IR (KBr; cm⁻¹): 3067, 1627, 1586, 1488, 1189, 1086, 845, 776, 699. Anal. calc. for C₁₉H₁₃Cl₄CoN₃ (484.07): C, 47.14; H, 2.71; N, 8.68. Found: C, 47.11; H, 2.70; N, 8.62.

[N,N'-Bis(4-chloro-2,6-dimethylphenyl)pyridine-2,6-carboximidoyl dichloride] CoCl₂ (4e)]. Yield, 0.53 g (86.9%). FT-IR (KBr; cm⁻¹): 3084, 2955, 1625, 1587, 1469, 1177, 1080, 950, 861, 799, 630. Anal. calc. for C₂₃H₁₉Cl₆CoN₃ (609.07): C, 45.36; H, 3.14; N, 6.90. Found: C, 45.31; H, 3.11; N, 6.88.

2,6-Bis[1-(2,4,6-trimethylphenylimino)ethyl]pyridine CoCl₂ (5a)]. 2,6-Diacetylpyridine (0.98 g, 6 mmol) and 2,4,6-trimethylaniline (1.69 g, 12.5 mmol) were added to a flask containing ethanol (40 mL) and formic acid (0.2 mL). The reaction mixture was stirred for 48 h at room temperature. A saturated solution was obtained by evaporating ethanol. The solution was kept at -40 °C for 48 h, and yellow crystals were obtained. The crystals were washed with cold methanol and dried under vacuum at 40 °C. Yield, 2.18 g (91.7%). ¹H NMR (400 MHz, CDCl₃, δ, ppm): 8.47 (d, 2H, Pyr-*H_m*), 7.90 (t, 1H, Pyr-*H_o*), 6.90 (s, 4H, Ar-H), 2.30 (s, 6H, Ar-C_PH₃), 2.0 (s, 12H, Ar-C_OH₃). FT-IR (KBr; cm⁻¹): 3005, 2974, 1637, 1569, 1479, 1364, 1214, 1118, 854, 820, 561. Anal. calc. for C₂₇H₃₁N₃ (397.6): C, 81.57; H, 7.86; N, 10.57. Found: C, 81.64; H, 7.95; N, 10.66.

2,6-Bis[1-(2,4,6-trimethylimino)ethyl]pyridine (0.40 g, 1.0 mmol) and CoCl₂ (0.13 g, 1.0 mmol) were added to a flask containing 5 mL THF. The reaction mixture was stirred for 4 h and a green suspension was formed. 20 mL Et₂O was added to the suspension and a green powder was obtained by filtration. The product was dried under vacuum at 40 °C. Yield, 0.49 g (92.4%). A single crystal of **5a** was obtained by layering *n*-pentane on their dichloromethane solutions at room temperature. FT-IR (KBr; cm⁻¹): 3031, 2975, 1636, 1583, 1478, 1369, 1262, 1223, 1064, 860, 570. Anal. calc. for C₂₇H₃₁Cl₂CoN₃ (526.4): C, 61.49; H, 5.92; N, 7.97. Found: C, 61.45; H, 5.88; N, 7.89.

General procedure for 1,3-butadiene solution polymerization

A typical procedure for the polymerization is as follows (entry 1 in Table 3): a toluene solution of 1,3-butadiene (20 mL, 0.1 g mL⁻¹) was added to a moisture free ampule preloaded with complex **4a** (7 mg, 12.3 μmol), and then EASC (0.62 mmol) was injected to initiate the polymerization at 20 °C. After 20 min, methanol was added to quench the polymerization. The mixture was poured into a large amount of methanol containing 2,6-di-*tert*-butyl-4-methylphenol (1.0 wt%) as a stabilizer. The precipitated polymer was washed with methanol, and then dried under vacuum at 40 °C to constant weight. The polymer yield was determined by gravimetry.

X-ray crystallographic studies

Crystals for X-ray analyses were obtained as described in the Experimental section. Data collections were performed at low or room temperature on a Bruker SMART APEX diffractometer

with a CCD area detector using graphite monochromated MoK radiation ($\lambda = 0.71073 \text{ \AA}$). The determination of crystal class and unit cell parameters was carried out using the SMART program package. The raw frame data were processed using SAINT and SADABS to yield the reflection data file. The structures were solved using the SHELXTL program. Refinement was performed on F^2 anisotropically for all non-hydrogen atoms by the full-matrix least-squares method. The hydrogen atoms were placed at the calculated positions and were included in the structure calculation without further refinement of the parameters. Details of X-ray structure determinations and refinements are provided in Table S1 in the ESI.† CCDC 872215, 903515 to 903517, 941866 to 941867.

Acknowledgements

The authors appreciate financial support from the National Science and Technology Infrastructure Program (2007BAE14B01-06), the Fund for Creative Research Groups (50621302) and the National Natural Scientific Foundation of China (no. 20974016).

Notes and references

- G. Ricci, A. Sommazzi, F. Masi, M. Ricci, A. Boglia and G. Leone, *Coord. Chem. Rev.*, 2010, **254**, 661–676; L. Porri, A. Giarrusso and G. Ricci, *Prog. Polym. Sci.*, 1991, **16**, 405–441; L. Friebe, O. Nuyken and W. Obrecht, in *Neodymium Based Ziegler Catalysts – Fundamental Chemistry*, ed. O. Nuyken, Springer Berlin Heidelberg, 2006, vol. 204, pp. 1–154; S. K. H. Thiele and D. R. Wilson, *J. Macromol. Sci., Polym. Rev.*, 2003, **C43**, 581–628.
- G. Ricci, C. Bosisio and L. Porri, *Macromol. Rapid Commun.*, 1996, **17**, 781–785; A. van der Linden, C. J. Schaverien, N. Meijboom, C. Ganter and A. G. Orpen, *J. Am. Chem. Soc.*, 1995, **117**, 3008–3021.
- Y. Nakayama, Y. Baba, H. Yasuda, K. Kawakita and N. Ueyama, *Macromolecules*, 2003, **36**, 7953–7958; G. Ricci, D. Morganti, A. Sommazzi, R. Santi and F. Masi, *J. Mol. Catal. A: Chem.*, 2003, **204**, 287–293.
- Y. Jang, D. S. Choi and S. Han, *J. Polym. Sci., Part A: Polym. Chem.*, 2004, **42**, 1164–1173; J. Furukawa, *Pure Appl. Chem.*, 1975, **42**, 495–508.
- S. Sivaram and V. K. Upadhyay, *J. Macromol. Sci., Pure Appl. Chem.*, 1992, **29**, 13–19; H. Ashitaka, H. Ishikawa, H. Ueno and A. Nagasaka, *J. Polym. Sci., Part A: Polym. Chem.*, 1983, **21**, 1853–1860; G. Ricci, A. Forni, A. Boglia, T. Motta, G. Zannoni, M. Canetti and F. Bertini, *Macromolecules*, 2005, **38**, 1064–1070; D. C. D. Nath, T. Shiono and T. Ikeda, *Appl. Catal., A*, 2003, **238**, 193–199.
- L. Zhang, T. Suzuki, Y. Luo, M. Nishiura and Z. Hou, *Angew. Chem., Int. Ed.*, 2007, **46**, 1909–1913; Z. Zhang, D. Cui, B. Wang, B. Liu and Y. Yang, *Struct. Bonding*, 2010, **137**, 49; L. Zhang, Y. Luo and Z. Hou, *J. Am. Chem. Soc.*, 2005, **127**, 14562–14563; L. Zhang, M. Nishiura, M. Yuki, Y. Luo and Z. Hou, *Angew. Chem., Int. Ed.*, 2008, **47**, 2642–2645.
- D. C. D. Nath, T. Shiono and T. Ikeda, *Macromol. Chem. Phys.*, 2002, **203**, 756–760; K. Endo and N. Hatakeyama, *J. Polym. Sci., Part A: Polym. Chem.*, 2001, **39**, 2793–2798; G. Ricci, A. Forni, A. Boglia, A. Sommazzi and F. Masi, *J. Organomet. Chem.*, 2005, **690**, 1845–1854; Y. Jang, P. Kim and H. Lee, *Macromolecules*, 2002, **35**, 1477–1480; D. Gong, X. Jia, B. Wang, X. Zhang and L. Jiang, *J. Organomet. Chem.*, 2012, **702**, 10–18.
- G. J. P. Britovsek, M. Bruce, V. C. Gibson, B. S. Kimberley, P. J. Maddox, S. Mastroianni, S. J. McTavish, C. Redshaw, G. A. Solan, S. Stromberg, A. J. P. White and D. J. Williams, *J. Am. Chem. Soc.*, 1999, **121**, 8728–8740; V. C. Gibson, C. Redshaw and G. A. Solan, *Chem. Rev.*, 2007, **107**, 1745–1776; J. Liu, Y. Li, J. Liu and Z. Li, *Macromolecules*, 2005, **38**, 2559–2563; W. Zhang, W. Chai, W.-H. Sun, X. Hu, C. Redshaw and X. Hao, *Organometallics*, 2012, **31**, 5039–5048; J. D. A. Pelletier, Y. D. M. Champouret, J. Cadarso, L. Clowes, M. Gañete, K. Singh, V. Thanarajasingham and G. A. Solan, *J. Organomet. Chem.*, 2006, **691**, 4114–4123.
- R. Cariou, J. J. Chirinos, V. C. Gibson, G. Jacobsen, A. K. Tomov, G. J. P. Britovsek and A. J. P. White, *Dalton Trans.*, 2010, **39**, 9039–9045.
- P. Ai, L. Chen, Y. Guo, S. Jie and B.-G. Li, *J. Organomet. Chem.*, 2012, **705**, 51–58.
- Y. Nakayama, K. Sogo, Z. Cai, H. Yasuda and T. Shiono, *Polym. Int.*, 2011, **60**, 692–697.
- D. Gong, B. Wang, C. Bai, J. Bi, F. Wang, W. Dong, X. Zhang and L. Jiang, *Polymer*, 2009, **50**, 6259–6264; D. Gong, B. Wang, H. Cai, X. Zhang and L. Jiang, *J. Organomet. Chem.*, 2011, **696**, 1584–1590.
- G. J. P. Britovsek, S. A. Cohen, V. C. Gibson, P. J. Maddox and M. van Meurs, *Angew. Chem., Int. Ed.*, 2002, **41**, 489–491; B. L. Small, M. Brookhart and A. M. A. Bennett, *J. Am. Chem. Soc.*, 1998, **120**, 4049–4050.
- S. Nüchel and P. Burger, *Organometallics*, 2001, **20**, 4345–4359; G. Zohuri, S. Seyedi, R. Sandaroods, S. Damavandi and A. Mohammadi, *Catal. Lett.*, 2010, **140**, 160–166; F. Pelascini, M. Wesolek, F. Peruch and P. J. Lutz, *Eur. J. Inorg. Chem.*, 2006, **2006**, 4309–4316.
- Z. Ma, W. H. Sun, Z. L. Li, C. X. Shao, Y. L. Hu and X. H. Li, *Polym. Int.*, 2002, **51**, 994–997.
- K. P. Tellmann, V. C. Gibson, A. J. P. White and D. J. Williams, *Organometallics*, 2005, **24**, 280–286.
- V. C. Gibson, N. J. Long, P. J. Oxford, A. J. P. White and D. J. Williams, *Organometallics*, 2006, **25**, 1932–1939; A. S. Ionkin, W. J. Marshall, D. J. Adelman, B. B. Fones, B. M. Fish and M. F. Schifffhauer, *Organometallics*, 2006, **25**, 2978–2992.
- C. Liu and G. Jin, *New J. Chem.*, 2002, **26**, 1485–1489; Z. Zheng, J. Chen and Y. Li, *J. Organomet. Chem.*, 2004, **689**, 3040–3045; B. L. Small and M. Brookhart, *J. Am. Chem. Soc.*, 1998, **120**, 7143–7144; J. Lai, W. Zhao, W. Yang, C. Redshaw, T. Liang, Y. Liu and W.-H. Sun, *Polym. Chem.*,

- 2012, **3**, 787–793; J. Yu, W. Huang, L. Wang, C. Redshaw and W. Sun, *Dalton Trans.*, 2011, **40**, 10209–10214.
- 19 A. S. Ionkin, W. J. Marshall, D. J. Adelman, A. L. Shoe, R. E. Spence and T. Xie, *J. Polym. Sci., Part A: Polym. Chem.*, 2006, **44**, 2615–2635; C. Görl and H. G. Alt, *J. Organomet. Chem.*, 2007, **692**, 4580–4592.
- 20 T. M. Smit, A. K. Tomov, G. J. P. Britovsek, V. C. Gibson, A. J. P. White and D. J. Williams, *Catal. Sci. Technol.*, 2012, **2**, 643–655.
- 21 S. Damavandi, G. Zohuri, R. Sandaroos and S. Ahmadjo, *J. Polym. Res.*, 2012, **19**, 1–5; J. Y. Liu, Y. Zheng, Y. G. Li, L. Pan, Y. S. Li and N. H. Hu, *J. Organomet. Chem.*, 2005, **690**, 1233–1239; Y. Chen, R. Chen, C. Qian, X. Dong and J. Sun, *Organometallics*, 2003, **22**, 4312–4321.
- 22 K. Nomura, J. Y. Liu, S. Padmanabhan and B. Kitiyanan, *J. Mol. Catal. A: Chem.*, 2007, **267**, 1–29; H. H. Brintzinger, D. Fischer, R. Mulhaupt, B. Rieger and R. M. Waymouth, *Angew. Chem., Int. Ed.*, 1995, **34**, 1143–1170.
- 23 V. Appukkuttan, L. Zhang, C.-S. Ha and I. Kim, *Polymer*, 2009, **50**, 1150–1158.
- 24 G. Ricci, A. Forni, A. Boglia and T. Motta, *J. Mol. Catal. A: Chem.*, 2005, **226**, 235–241.
- 25 S. Jie, P. Ai and B. Li, *Dalton Trans.*, 2011, **40**, 10975–10982.